Current blockade in classical single-electron nanomechanical resonator

F. Pistolesi and S. Labarthe*
Laboratoire de Physique et Modélisation des Milieux Condensés, CNRS UMR 5493 and Université Joseph Fourier, 25 avenue des Martyrs, Boîte Postale 166, F-38042 Grenoble, France
(Received 21 July 2007; published 23 October 2007)

We consider a single-electron transistor where the central metallic island can oscillate. It has been shown that for a weak coupling of the elastic and electric degrees of freedom, the position of the island fluctuates with a small variation of the current through the device. In this paper, we consider the strong coupling limit. We show that the system undergoes a static mechanical instability that is responsible for the opening of a gap in the current-voltage characteristics even at the degeneracy point. We provide an analytical description of the transition point, taking into account the nonequilibrium mechanical state. We also discuss how the mechanical nature of the suppression of the current can be probed experimentally by a slow modulation of the gate voltage.

DOI: 10.1103/PhysRevB.76.165317 PACS number(s): 73.23.−b, 85.85.+j

I. INTRODUCTION

Nanoelectromechanics constitutes a rapidly developing and promising field of mesoscopic physics.[1–3] A particularly important and experimentally investigated device is the single-electron transistor with mobile parts.[4–7] Due to the Coulomb blockade, the interplay between the electrical and mechanical degrees of freedom influences the current in a sizable way. When the oscillation amplitude is sufficiently large with respect to the tunneling length, the modulation of the tunneling rates in metallic dots leads to the shuttle phenomena, where the oscillations become synchronized with the electron tunneling.[8–15] If the oscillation does not modify the distance between source and drain (for instance, for oscillations perpendicular to the source-drain line), it may, nevertheless, induce a modulation of the tunneling rates through the variation of the electric potential energy in space.[16–21] Typically, this effect is due to the position dependence of the gate capacitance. If the Coulomb force generated by the variation of the number of electrons by 1 is F, the distance of the two equilibrium positions of the island will be $X_o=F/k$, where k is the effective elastic constant of the island. The corresponding variation of the elastic energy is of the order of $F^2/k \equiv E_E$. For source-drain bias voltages V of the order of E_E/e (with e the electron charge), the interplay between the electrical and mechanical degrees of freedom becomes important. Typically, E_E is very small, but within the range of observation. For a nanotube of 500 nm length and 1 nm radius, suspended at 100 nm from a gate, E_E can be of the order of tens of μeV. Previous analytic work concentrates on the case $eV \gg E_E$.[17,22] Very recently, the current for $eV \geqslant E_E$ at the degeneracy point has been considered numerically.[21] In this paper, we present an analytic theory that gives a good description of the whole region $eV \geqslant E_E$ and arbitrary gate voltage taking into account the nonequilibrium state of the mechanical degrees of freedom. We find that sweeping the gate voltage for $eV > E_E$, the current shows a jump from 0 in the blocked regions to a finite value in the conducting regions. We also discuss the behavior of the system for $eV < E_E$. We argue how a static classical mechanical instability blocks the current for any value of the gate voltage. This effect can be regarded as the classical counterpart of the Franck-Condon blockade in the quantum limit that has been shown to lead to current suppression in molecular devices.[23–28] The fact that this phenomenon exists for systems with many electronic levels and that it survives in the classical limit opens new perspectives of experimental observation. Moreover, considering the classical limit allows us to obtain a transparent analytical solution and to treat complex situations, such as the nonstationary evolution discussed in the following.

The paper is organized as follows. In Sec. II, we describe the system discussed and its modelization. In Sec. III, we present a simple mean field description of the current blockade, neglecting both the fluctuation of the charge and of the position of the mobile part. In Sec. IV, we give an analytical description of the fluctuations. Specifically, we calculate the probability distribution for the energy. This allows us to obtain the current and the rms of the position. A comparison with a Monte Carlo simulation is also presented. In Sec. V, we show how the bistability can be probed by an oscillating gate voltage. Section VI gives our conclusions.

II. SYSTEM AND MODELIZATION

Let us consider a single-electron transistor with a mobile central island (see Fig. 1). The model has been discussed in detail in previous works (see, for instance, Refs. 17, 18, 20, and 21). We discuss the simplest configuration of symmetric capacitances, resistances, and bias. We also assume that E_E

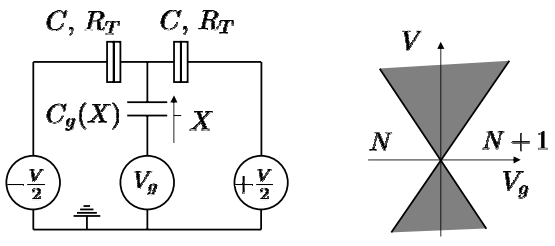

FIG. 1. Left panel: Circuit diagram for the single-electron transistor with an oscillating central island. The variable X parametrizes an effective position. Right panel: Conducting regions shaded in the V_g-V near a degeneracy point between N and $N+1$ electrons.

 ©2007 The American Physical Society

$\gg k_B T \gg \hbar\omega_o$: classical low temperature behavior. Here, ω_o is the oscillator frequency. For small oscillations, the gate capacitance varies linearly in the displacement of the island X. Charge transport can be described as usual by a master equation, where the rates are modulated by the position of the island. We discard in this paper cotunneling processes since their main effect is to induce a small current in the blocked regions. Far from the boundaries of the conducting region, this contribution is very small and can be safely neglected. Near the boundary on the blocked side, cotunneling can give a relevant contribution, and will be discussed elsewhere. For molecular devices, these processes have been very recently considered.[27,28] For positive source-drain voltage ($V>0$) smaller than the Coulomb energy E_C (defined below), and gate voltage V_g tuned close to the value for the states with N and $N+1$ electrons on the island to be degenerate, the only two nonvanishing rates read

$$\Gamma_{L,R} = -E_{L,R}(X)/e^2 R_T \quad \text{for } E_{L,R} < 0, \tag{1}$$

and zero otherwise. Here, Γ_L and Γ_R are the rates for the transfer of electrons from the left lead to the island and from the island to the right lead, respectively. R_T is the tunneling resistance of the left and right contacts. The rates are controlled by the Coulomb energy gain for tunneling:

$$E_{L,R}(X) = -(eV/2) \pm U(N+1,X) \mp U(N,X), \tag{2}$$

where

$$U(N,X) = E_C(X)N^2 - NeV_g C_g(X)/C_\Sigma(X), \tag{3}$$

with $E_C(X)=e^2/2C_\Sigma$ the Coulomb energy, $C_\Sigma(X)=2C+C_g(X)$, and, finally, C and $C_g(X)$ the junction and gate capacitances, respectively. For small displacements,

$$E_{L,R}(X) = E_{L,R}(0) \pm FX + \ldots, \tag{4}$$

where we defined

$$F = [dU(N+1,X)/dX] - [dU(N,X)/dX] \tag{5}$$

at $X=0$. If we choose $X=0$ as the position where the Coulomb force for N electrons in the island equals the elastic force, then $F>0$ is the net force (in the direction of negative X) acting on the mobile part when $N+1$ electrons are populating the island. For small variations of X, we can neglect the weak gate and bias voltage dependence of F that is assumed constant in the rest of the paper.

The motion of the island is described by the Newton equation:

$$m\ddot{X}(t) = -kX(t) - Fn(t), \tag{6}$$

where m is the effective mass of the island and $n(t)$ is the number of electrons on the island minus N. This quantity fluctuates stochastically between 0 and 1 according to the rates given by Eqs. (1) and (4). It has been shown that the coupling to the electronic degrees of freedom introduces an intrinsic damping coefficient.[17] We, thus, do not introduce an extrinsic dissipation into Eq. (6), assuming that the intrinsic dissipation is dominant. Adding an extrinsic dissipation does not change the complexity of the problem, since it is enough to add a term $-\eta\dot{X}(t)$ to Eq. (6) that will renormalize the intrinsic dissipation coefficient [see Eq. (11) in the following]. We prefer to consider the undamped case to keep the minimal number of parameters in the model. It is convenient to introduce now reduced variables:

$$x = X/X_o, \quad u = \dot{X}/\omega_o X_o, \quad \tau = \omega_o t,$$

$$v = eV/E_E, \quad v_g = [eV_g C/C_\Sigma(0) - (2N+1)E_C(0)]/E_E,$$

and

$$\Gamma_o = E_E/e^2 R_T \omega_o,$$

with $\omega_o^2 = k/m$ and $X_o = F/k$. For fixed x, the stationary current is given by the usual expression

$$\frac{R_T I}{V} = \frac{R_T e}{V}\frac{\Gamma_L\Gamma_R}{(\Gamma_L+\Gamma_R)} = \frac{(v^2/4) - (v_g - x)^2}{v^2}. \tag{7}$$

In the plane $v - v_g$, it leads to the Coulomb diamond structure of the current, as shown in Fig. 1, with the degeneracy point sitting at $v_g=0$ for $x=0$.

The effect of the oscillation of the central island on the current can be studied analytically far from the boundaries of the conducting regions.[17] In that limit, it has been shown that the probability distribution of x and u becomes Gaussian with a width controlled by the voltage bias v, and the variation of the current due to the mechanical coupling is always a small part of the unperturbed value. In this paper, we will focus on the regions near the degeneracy point and near the two lines of transition from the conducting to the nonconducting region (see Fig. 1, right panel). We assume that $\Gamma_o \gg 1$ so that the problem can be tackled by exploiting the separation of time scales between the slow mechanical oscillations and the frequent electronic hopping.

III. MEAN FIELD DESCRIPTION AND CURRENT BLOCKADE

We begin with a very simple description of the stochastic force by substituting into Eq. (6) the occupation number $n(t)$, with its average over a time short with respect to ω_o^{-1} and long with respect to the inverse of typical tunneling rate $\sim E_E/e^2 R_T$. This average depends only on the position of the mobile part: $\langle n(t)\rangle = \bar{n}(x)$, where

$$\bar{n}(x) = \begin{cases} (v/2 + v_g - x)/v & \text{for } |v_g - x| < v/2 \\ 0 & \text{for } v_g - x < -v/2 \\ 1 & \text{for } v_g - x > +v/2. \end{cases} \tag{8}$$

This induces an average force on the island that depends on the occupation of the island itself. It is convenient to introduce an effective potential to describe this force (in units of E_C):

$$U_{eff}(x) = \int_{x_m}^{x} [x + \bar{n}(x)]dx, \tag{9}$$

where $x_m = (v/2+v_g)/(1-v)$. The form of $\bar{n}(x)$ given above implies that d^2U_{eff}/dx^2 equals $(1-1/v)$ for $|v_g - x| < v/2$, and 1 otherwise. For $v>1$, the potential has, thus, a single

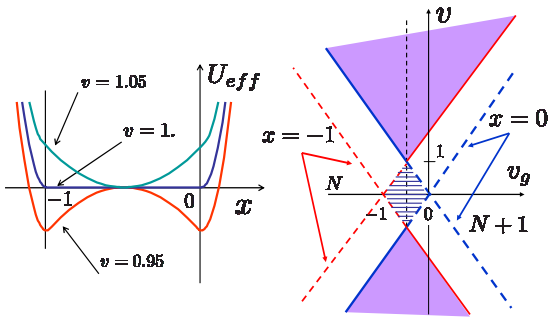

FIG. 2. (Color online) Left panel: Effective potential U_{eff} for $v_g=-1/2$ and $v=1.05$, 1, and 0.95. Right panel: Shape of the conducting regions (filled regions) in the plane v_g-v when the displacement of the mobile part is taken into account. The dashed lines indicate the border of the Coulomb diamonds for $x=0$ and $x=-1$. The small shaded diamond indicates the mechanically bistable region.

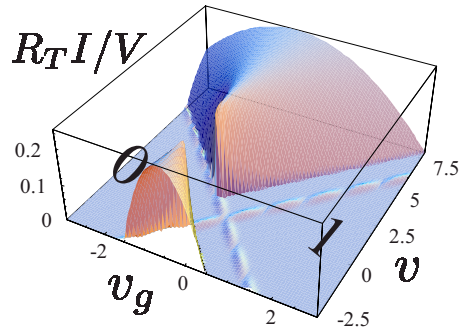

FIG. 3. (Color online) Current as a function of the reduced gate (v_g) and bias voltages (v) in the mean field approximation of Eq. (7) with $x=x_m$. The opening of a gap is clearly visible together with the fact that the current is continuous at the boundary of the conducting region. The border of the Coulomb diamonds for $x=0$ is shown dashed.

minimum at x_m, with $-1\leqslant x_m\leqslant 0$ and (by construction) $U_{eff}(x_m)=0$. For $0<v<1$, instead, two minima may be present, depending on the value of v_g. The evolution of the potential as a function of v is shown in Fig. 2 for $v_g=-1/2$. At $v=1$, the potential becomes flat, and for $v<1$, it develops two side minima.

The qualitative behavior of the device can now be understood in a very simple way. The crucial point is that the displacement of the average position acts as an effective positive shift of the gate voltage [cf. Eq. (8)]. This means that on the $v-v_g$ plane, the displacement of the oscillator of a unit distance (i.e., F/k) will induce a rigid shift of the current plot in v_g of 1 [i.e., $\Delta eV_g=E_E C_g/C_\Sigma$]. The blocked diamond with N electrons and undisplaced oscillator ($x=0$) will then overlap in the region $v<1$ with the blocked diamond with $N+1$ electrons and displaced oscillator ($x=-1$). The result is the presence of a mechanical bistable region (indicated in Fig. 2 by the dashed diamond), where current is always blocked. This effect corresponds to the classical limit of the Franck-Condon blockade (or phonon blockade) in molecular devices.[23,24,26–28] The simple argument given above applies quite generally, indicating that a current blockade near the degeneracy point should be a general feature of Coulomb blockade devices with mobile parts modulating the capacitances. The precise form of the current-voltage characteristics will then depend on the specific device, but the classical description gives a general and very simple view of the current blockade.

A plot of the current in the mean field approximation as a function of the gate and bias voltages is presented in Fig. 3. This plot reports simply Eq. (7) with $x=x_m$, i.e., with x at the stable position for $v>1$. The position of the Coulomb diamond for $x=0$ is also shown dashed for reference. Note that the current is always continuously vanishing at the border of the conducting region in this approximation.

IV. ANALYTICAL DESCRIPTION OF THE FLUCTUATIONS IN PHASE SPACE

Let us now discuss the behavior of the system in the conducting region ($v>1$). The dependence of the current and the probability distribution on x along the degeneracy line ($v_g=-1/2$ and $v>1$) has been considered very recently in Ref. 21 numerically. We present here an analytical theory that gives a good description of the current in the whole conducting region, including near the boundaries and at the apex. For $\Gamma_o\gg 1$, the electrons have the time to hop in and out of the grain many times before it can move a sizable distance. One can then write a Fokker-Planck equation for the probability $\mathcal{Q}(x,u)$ of finding the mobile part at a given position x with a velocity[18,20,27] u

$$\frac{\partial \mathcal{Q}}{\partial t}=-\frac{\partial}{\partial u}[F_e(x)-\eta_i(x)u]\mathcal{Q}-\frac{\partial}{\partial x}u\mathcal{Q}+\frac{1}{2}\frac{\partial}{\partial u^2}S(x)\mathcal{Q}, \tag{10}$$

where $F_e(x)=-dU_{eff}/dx$, and

$$\eta_i(x)=\frac{1}{v\Gamma_o}\frac{\partial \bar{n}}{\partial v_g} \tag{11}$$

is the intrinsic damping.[17,20] The nonvanishing second moment is

$$S(x)=\int_{-\infty}^{+\infty}d\tau\langle\delta n(\tau)\delta n(0)\rangle=\frac{2\bar{n}(x)[1-\bar{n}(x)]}{\Gamma_o v}, \tag{12}$$

where $\delta n(\tau)=n(\tau)-\langle n(t)\rangle$.

It is convenient to simplify further the equation by exploiting the fact that the fluctuating and dissipative part is small for $\Gamma_o\gg 1$. One can then expect that the system performs many oscillations following the same isoenergetic trajectory in the phase space before slowly drifting away on another nearby trajectory. The distribution function will, thus, depend on the position and the velocity mainly through the effective energy:

$$E_e(x,u)=U_{eff}(x)+u^2/2. \tag{13}$$

If we define the function

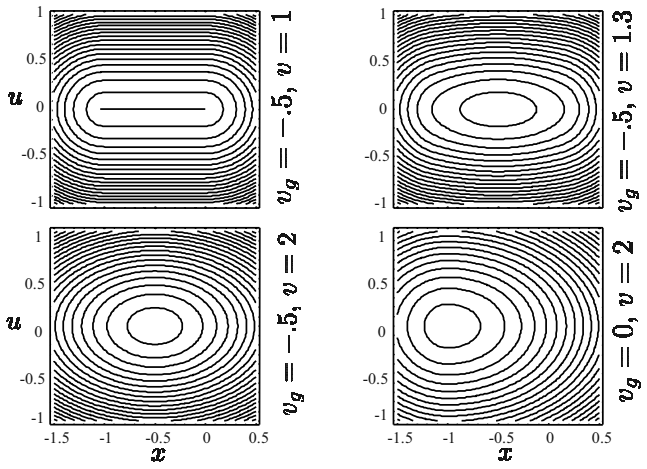

FIG. 4. Lines of equal energy and, thus, of equal probability $\mathcal{Q}$ in the $x-u$ plane for the values of v and v_g indicated.

$$\mathcal{P}(E) \equiv \int dxdu\mathcal{Q}(x,u)\delta[E - E_e(x,u)], \tag{14}$$

we can then derive from Eq. (10) an equation for it:

$$\frac{\partial \mathcal{P}}{\partial t} = \frac{\partial}{\partial E}\left[-\alpha(E)\mathcal{P}(E) + \frac{\partial}{\partial E}[\beta(E)\mathcal{P}(E)]\right], \tag{15}$$

with

$$\alpha(E) = \langle S(x)/2 - \eta_i(x)u^2\rangle_E, \tag{16}$$

$$\beta(E) = \langle S(x)u^2/2\rangle_E, \tag{17}$$

where the averages are taken on the trajectories in the $x-u$ plane at fixed energy E. These trajectories are shown for some values of v and v_g in Fig. 4. Near the apex and the borders, the shape is quite different from an ellipse, which is the harmonic oscillator trajectory.

The stationary solution of Eq. (15) is

$$\mathcal{P}(E) = \mathcal{N}\exp\left\{\int^E dE'\,\alpha(E')/\beta(E')\right\}\Big/\,\beta(E), \tag{18}$$

where $\mathcal{N}$ is a normalization constant. Once $\mathcal{P}(E)$ is known, the relevant physical quantities can be calculated by averaging, first, over the trajectories, and then over the energy.

A. Current and position fluctuations at the apex of the conducting region

Let us now test the theory at the strongest value of the interaction, at the apex of the new Coulomb diamond: $v=1$ and $v_g=-1/2$. The orbits are quite simple for this case (see Fig. 4). The velocity is constant for $|x+1/2|<1/2$, and the trajectory is exactly half an ellipse for $|x+1/2|>1/2$. The averages of η_i and S on this trajectories lead to the following expressions for α and β:

$$\alpha = \frac{\bar{S}/2 - 2\bar{\eta}_i E}{(1+\pi\sqrt{2E})}, \quad \beta = \frac{\bar{S}E}{2(1+\pi\sqrt{2E})}, \tag{19}$$

where $\bar{S}=1/3\Gamma_o$ and $\bar{\eta}_i=1/\Gamma_o$ are the averages of $S(x)$ and $\eta_i(x)$, respectively, on the segment $-1<x<0$. This leads to the probability

$$\mathcal{P}(E) = \mathcal{N}(1+\pi\sqrt{2E})e^{-6E}/\sqrt{E}. \tag{20}$$

The current at the apex can be obtained by integrating expression (7) with the distribution (20) [and using Eq. (14)]. We find that

$$\frac{R_T}{V}I(v=1, v_g=-1/2) = \frac{1}{6+2\sqrt{3\pi}} \approx 0.0837. \tag{21}$$

With the same technique, one can calculate the rms of x:

$$(\langle (x-\bar{x})^2\rangle)^{1/2} = \left(\frac{40+3\sqrt{6}\pi^{3/2}}{96+8\sqrt{6}\pi^{3/2}}\right)^{1/2} \approx 0.628. \tag{22}$$

It is interesting to notice that the current-voltage curves, once rescaled with V/R_T, become universal in the limit of large Γ_o.

B. Current and position fluctuations at the border of the conducting region

The method can be applied to describe the transition from the blocked to the conducting state at finite v. In order to keep the calculation simple, we consider $v \gg 1$. For $v_g=-v/2$, the minimum of the potential is at $x=0$. The potential is harmonic for $x<0$ with oscillation period 2π, and harmonic for $x>0$ with period $2\pi(1-1/v)^{-1/2}$. The oscillations will, thus, be more elongated inside the conducting regions (see Fig. 4). The calculation at leading order in $1/v$ gives the distribution

$$\mathcal{P}(E) = \mathcal{N}\left[1 - \frac{3\pi\sqrt{E}}{8v\sqrt{2}(1-1/v)^{1/2}}\right]^{4(1-1/v)v}. \tag{23}$$

With this distribution, we find that the current jumps at $v_g=-v/2$ (and symmetrically at $v_g=-v/2-1$) with

$$\frac{R_T}{V}I(v, v_g=-v/2^+) = \frac{8}{3\pi^2 v}\left[1 - \frac{1}{2v} - \frac{1}{4v^2} + o(v^{-3})\right].$$

For arbitrary values of v_g and v, we found the analytical expressions for α and β, and they have been used to obtain the current by numerical integration. We do not give the details of the calculation that is trivial, but rather tedious. One has to calculate the averages of α and β on trajectories that are composed of arcs of ellipses matched at the boundaries of the segment $-1<x<0$.

The results for the current are presented in Figs. 5 and 6. The features discussed above are clearly visible in Fig. 5: the discontinuity of the current at the threshold, and the opening of the gap. It is also evident that the current flattens as a function of v_g with respect to the mean field approximation. This can be seen even more clearly in Fig. 6, which shows a

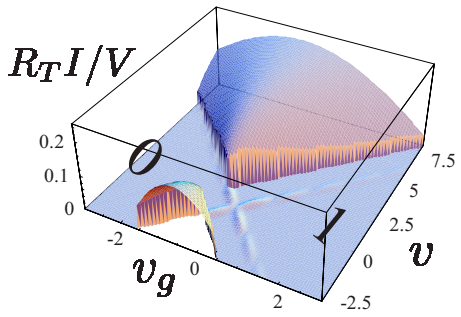

FIG. 5. (Color online) Current as a function of v_g and v, including the effect of position fluctuation. The dependence on v_g is reduced inside the conducting region with respect to the mean field result due to the average over the different positions visited by the oscillating part.

comparison of the contour plot of the current for the mean field results and the fluctuation corrected ones.

C. Probability distribution for the position

From the form of $\mathcal{P}(E)$, one can easily obtain the probability distribution for the position $P(x)$:

$$P(x) = \int_0^\infty \mathcal{P}(E)dE \int_0^{T(E)} \delta[x - x_E(t)] \frac{dt}{T(E)}. \tag{24}$$

Here, $T(E)$ is the period of the trajectory, and $x_E(t)$ is the trajectory as a function of time for a given energy E. At the apex of the conducting region, $P(x)$ takes a particularly simple form (Fig. 7)

$$P(x) = \int_0^\infty \mathcal{P}(E)dE \begin{cases} \dfrac{2}{\sqrt{2E}} \dfrac{1}{T(E)} & \text{for } -1 < x < 0 \\ \dfrac{2}{T(E)} \dfrac{\theta(2E - x^2)}{\sqrt{2E - x^2}} & \text{for } 0 < x < \sqrt{2E}, \end{cases} \tag{25}$$

where $T(E) = 2\pi + \sqrt{2/E}$ is the period of the oscillation in our units, and θ is the Heaviside function. As can be seen from Fig. 7, the probability is symmetric with respect to the value $x = -1/2$. The mobile part moves at a constant velocity inside

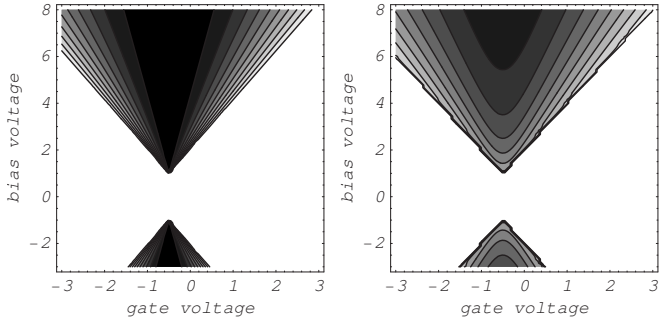

FIG. 6. Comparison of the contour plots of the current in mean field approximation (left) and taking into account the fluctuations (right) as a function of the gate (v_g) and bias voltage (v).

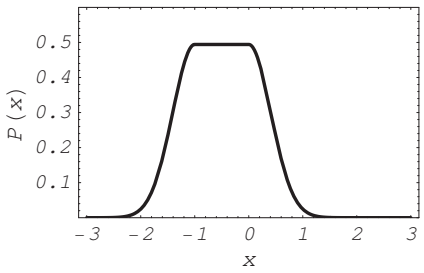

FIG. 7. Probability distribution for the position at the apex of the conducting region.

the region $-1 < x < 0$ for any value of the energy E, thus the probability is flat in that region. It then decays on a scale of X_o symmetrically. A comparison with the numerical simulations of Ref. 21 shows that the analytical approximation is accurate, apart from a small region around $x = 0$ and $x = -1$, where it is not able to reproduce the narrow peak precursors of the bistability.

D. Comparison with Monte Carlo simulation

To check these results, we have performed a Monte Carlo simulation of the model (see, for instance, Refs. 13 and 21). Figure 8 shows the comparison for $v_g = -1/2$ and v varied between 0 and 8, and for fixed $v = 1.5$ and v_g varied between the blocked region to the degeneracy point (inset). We considered values Γ_o ranging from 10^{-2} to 10. Surprisingly, the agreement between the analytical and the numerical calculations is very good also for $\Gamma_o \ll 1$. Apparently, the current depends very weakly on Γ_o (apart from a trivial linear scaling).

Concerning the v_g dependence of the current, the inset of Fig. 8 on top of the Monte Carlo results presents a comparison between (i) the analytical results (full line, partially hid-

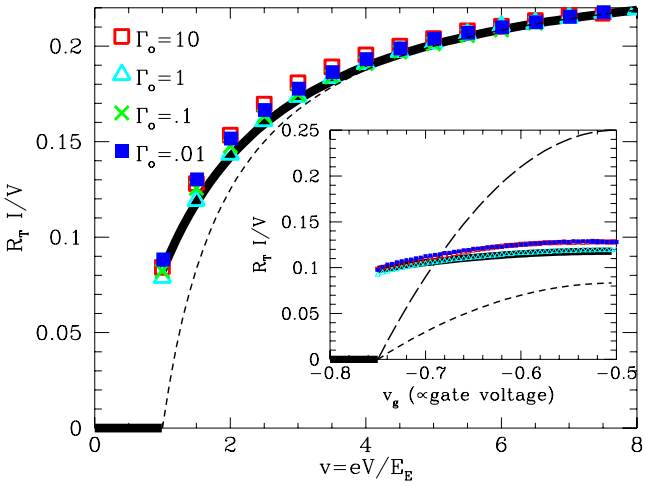

FIG. 8. (Color online) Current as a function of v at $v_g = -1/2$ from the analytical calculation (solid line), the weak coupling theory (dashed line), and the Monte Carlo simulation (points). The values of Γ_o are 10 (empty square), 1 (triangle), 0.1 (cross), and 0.01 (filled square). Inset: Current as a function of v_g for $v = 1.5$. The long dashed line is Eq. (7) for $x = x_m$.

den by the Monte Carlo points), (ii) the weak coupling results of Ref. 17 extrapolated to strong coupling (dashed line), and (iii) expression (7) taken at $x=x_m$ (long dashed line). For $v_g > -v/2$, the current flows through the device, inducing a fluctuation of the position. The observed current is then the average of Eq. (7) over the values of x visited by the island. This average increases the current near the threshold, producing the discontinuity, and reduces it near the degeneracy point. Also, for the rms of the position, the analytical estimate given above agrees with the numerical simulation: for Γ_o varying in the same range of Fig. 8, we find that $\sqrt{\langle (x-\bar{x})^2 \rangle}$ ranges between 0.59 and 0.64, which compares well with the analytical result of 0.628. The good agreement between the analytical and Monte Carlo results indicates that the analytical picture is accurate. It, thus, provides a simple and faithful description of device dynamics.

V. PROBING THE BISTABILITY BY GATE VOLTAGE MODULATION

The presence of the mechanical bistability can be experimentally probed for $v<1$ by modulating the gate voltage around $-1/2$: $v_g=-1/2+v_g^o \sin(\omega t)$. According to the picture given before, if $v_g^o < (1-v)/2$, no current should flow since the island remains in the same stable or metastable position all the time: v_g varies inside the dashed diamond of Fig. 2. For $v_g^o > (1-v)/2$, the island is instead always released from the metastable state, and it is free to oscillate between the two positions $x=-1$ and $x=0$. This implies that some current can flow through the device. The resulting average current as a function of v_g^o is, thus, discontinuous at $v_g^o=(1-v)/2$. In order to verify this idea quantitatively, we resort to a Monte Carlo simulation for this nonstationary situation. Results are shown in Fig. 9 for $v=1/2$ and $\omega/\omega_o=0.1$. For $v_g^o \gg (1-v)/2=1/4$, we find that the current is one electron per cycle, regardless of the value of Γ_o. The value of the discontinuity depends instead strongly on Γ_o. For $\Gamma_o \gg 1$, many electrons can flow during the swing of the oscillator between the two stable solutions. In the opposite limit of $\Gamma_o \ll 1$, the discontinuity is strongly reduced. Nevertheless, also in this case, the nanomechanical nature of the current can be probed by studying the average current as a function of the external frequency ω/ω_o. The inset shows the frequency dependence of the current at the threshold ($v_g^o=1.05/4$) for large and small Γ_o. In both cases, dips are present when $\omega/\omega_o=0.5$, 1, or 2, indicating the resonant response of the mechanical degree of freedom.

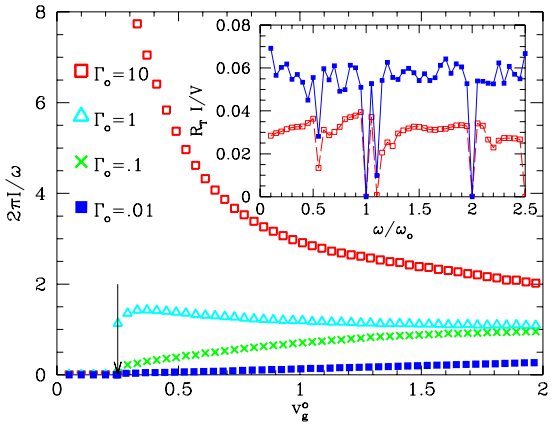

FIG. 9. (Color online) Average current response to an oscillating gate voltage $v_g=-1/2+v_g^o \sin(\omega t)$ as a function of v_g^o. $v=1/2$ and $\omega/\omega_o=0.1$ (same symbols as in Fig. 8). The arrow indicates the threshold to the conducting region. Inset: Frequency dependence of the average current for $v_g^o=1.05$ the threshold value. Structures at $\omega/\omega_o=0.5$, 1, and 2 are clearly visible.

VI. CONCLUSIONS

In conclusion, we have shown that the coupling to a classical mechanical degree of freedom can lead to a current suppression at the degeneracy point. The effect is expected to be quite a general feature of Coulomb blockade devices, thus expected also, for instance, in classical or quantum superconducting devices. It is associated with a mechanical bistability appearing for $eV<E_E$. We have shown how this can be detected by using an ac gate voltage, and presented an analytic theory that allows us to calculate with quantitative accuracy the current in the whole conducting region ($eV>E_E$). A gap at the degeneracy point has been already observed experimentally in different nanomechanical devices.[4,24] The miniaturization of the devices will allow us to increase further the value of E_E. Our predictions can be useful to test whether the observed phenomena are really related to nanomechanical effects.

ACKNOWLEDGMENTS

We acknowledge discussions with A. D. Armour, C. B. Doiron, L. Duraffourg, D. Feinberg, F. Hekking, M. Houzet, and I. Martin. We acknowledge support from the French Agence Nationale Recherche (Project No. JCJC06-NEMESIS) and IdNano (Grenoble).

*Present address: Laboratoire des Composantes Microsystèmes, CEA/LETI-MINATEC, 38054 Grenoble, France.

[1] M. Roukes, Phys. World **14** (2), 25 (2001).
[2] A. Cleland and M. Roukes, Nature (London) **392**, 160 (1998).
[3] M. P. Blencowe, Phys. Rep. **395**, 159 (2004).
[4] H. Park, J. Park, A. Lim, E. Anderson, A. Alivisatos, and P. McEuen, Nature (London) **407**, 57 (2000).
[5] V. Sazonova, Y. Yaish, H. Ustunel, D. Roundy, A. Arias, and P. M. McEuen, Nature (London) **431**, 284 (2004).
[6] S. Sapmaz, P. Jarillo-Herrero, Y. M. Blanter, C. Dekker, and H. S. J. van der Zant, Phys. Rev. Lett. **96**, 026801 (2006).
[7] A. Naik, O. Buu, M. D. LaHaye, A. D. Armour, A. A. Clerk, M. P. Blencowe, and K. C. Schwab, Nature (London) **443**, 193 (2006).

[8] L. Y. Gorelik, A. Isacsson, M. V. Voinova, B. Kasemo, R. I. Shekhter, and M. Jonson, Phys. Rev. Lett. **80**, 4526 (1998).
[9] A. D. Armour and A. MacKinnon, Phys. Rev. B **66**, 035333 (2002).
[10] T. Novotny, A. Donarini, C. Flindt, and A.-P. Jauho, Phys. Rev. Lett. **92**, 248302 (2004).
[11] F. Pistolesi, Phys. Rev. B **69**, 245409 (2004).
[12] D. Scheible and R. Blick, Appl. Phys. Lett. **84**, 4632 (2004).
[13] F. Pistolesi and R. Fazio, Phys. Rev. Lett. **94**, 036806 (2005).
[14] L. M. Jonsson, L. Y. Gorelik, R. I. Shekhter, and M. Jonson, Nano Lett. **5**, 1165 (2005).
[15] F. Pistolesi and R. Fazio, New J. Phys. **8**, 113 (2006).
[16] N. M. Chtchelkatchev, W. Belzig, and C. Bruder, Phys. Rev. B **70**, 193305 (2004).
[17] A. D. Armour, M. P. Blencowe, and Y. Zhang, Phys. Rev. B **69**, 125313 (2004).
[18] Ya. M. Blanter, O. Usmani, and Y. V. Nazarov, Phys. Rev. Lett. **93**, 136802 (2004); **94**, 049904(E) (2005).
[19] A. A. Clerk and S. Bennet, New J. Phys. **7**, 238 (2005).
[20] O. Usmani, Y. M. Blanter, and Y. V. Nazarov, Phys. Rev. B **75**, 195312 (2007).
[21] C. B. Doiron, W. Belzig, and C. Bruder, Phys. Rev. B **74**, 205336 (2006).
[22] A. D. Armour, Phys. Rev. B **70**, 165315 (2004).
[23] S. Braig and K. Flensberg, Phys. Rev. B **68**, 205324 (2003).
[24] E. M. Weig, R. H. Blick, T. Brandes, J. Kirschbaum, W. Wegscheider, M. Bichler, and J. P. Kotthaus, Phys. Rev. Lett. **92**, 046804 (2004).
[25] A. Mitra, I. Aleiner, and A. J. Millis, Phys. Rev. B **69**, 245302 (2004).
[26] J. Koch and F. von Oppen, Phys. Rev. Lett. **94**, 206804 (2005).
[27] D. Mozyrsky, M. B. Hastings, and I. Martin, Phys. Rev. B **73**, 035104 (2006).
[28] J. Koch, F. von Oppen, and A. V. Andreev, Phys. Rev. B **74**, 205438 (2006).